Polymer Journal (2019) 51:1137–1146
https://doi.org/10.1038/s41428-019-0227-y

ORIGINAL ARTICLE

Role of N-substituents of maleimides on penultimate unit effect for sequence control during radical copolymerization

Suguru Terada[1] · Akikazu Matsumoto[1]

Received: 27 March 2019 / Revised: 5 June 2019 / Accepted: 8 June 2019 / Published online: 8 July 2019

Abstract

Radical copolymerization of N-substituted maleimides (RMIs) and olefins provides AAB sequence-controlled copolymers by penultimate unit (PU) control. In this study, we investigated the steric, resonance, and polar effects of N-substituents on sequence control during copolymerization of RMIs as the M_2 monomer with diisobutene (DIB) and *d*-limonene (Lim) as the M_1 monomer in chloroform at 60 °C. The monomer reactivity ratios (i.e., r_2 ($=k_{22}/k_{21}$), r_{12} ($=k_{122}/k_{121}$), and r_{22} ($=k_{222}/k_{221}$)) were determined based on the terminal and PU models using a nonlinear least-squares method. For the copolymerization of RMIs with DIB, the introduction of a bulky *N*-alkyl group suppressed the PU effect and led to the formation of alternating copolymers. The copolymerization of *N*-phenylmaleimides with *o*- and *p*-substituents was also investigated to reveal the steric, resonance, and polar effects of the substituents. In conclusion, less bulky and more electron-donating substituents effectively induced the PU effect during the radical copolymerization of RMIs and olefins.

Introduction

Radical polymerization is advantageous for producing a large quantity of polymers from inexpensive vinyl monomers under mild conditions. Therefore, this approach is the most popular for the industrial production of polymers. The control of the molecular weight, molecular weight distribution and chain-end structures of polymers has been achieved by the development of living radical polymerizations during the past two decades [1–6]. In addition, polymer architectures can be designed with a precisely controlled structure using living radical polymerization [7–11]. Stereocontrol (i.e., tacticity of the polymers) via radical polymerization was also achieved via the addition of a Lewis acid and a selection of solvents [12, 13].

For a long time, many efforts focused on the synthesis of polymers with a complex structure through radical polymerization. Recently, much interest has turned to the sequence control of polymers using living radical polymerization [14–19], template polymerization [20–22], and predesigned reactive oligomers [23–25]. Radical alternating copolymerization is the oldest and simplest example of sequence-controlled polymerization [26, 27]. When an electron-accepting monomer and an electron-donating monomer are coupled, an alternating copolymer with a high molecular weight is readily produced in a high yield via a radical polymerization process in the presence or absence of a radical initiator. Alternating copolymerization is enhanced by a lack of homopolymerization ability of either or both monomers used for copolymerization. N-substituted maleimides (RMIs), which are the typical electron-accepting monomers, provide alternating copolymers by combination with olefins, styrenes, and vinyl ethers as the electron-donating counterparts [28–33]. The obtained copolymers exhibit a high onset temperature for thermal decomposition (T_{d5}) and a high glass transition temperature (T_g) due to the stable imide ring and rigid poly(substituted methylene) structures in the main chain [32]. For example, the alternating copolymer consisting of *N*-methylmaleimide (MMI) and isobutene is highly heat resistant (T_{d5} more than 350 °C and T_g more than 150 °C) (Scheme 1) [33]. In addition, this copolymer possesses excellent optical

Supplementary information The online version of this article (https://doi.org/10.1038/s41428-019-0227-y) contains supplementary material, which is available to authorized users.

✉ Akikazu Matsumoto
matsumoto@chem.osakafu-u.ac.jp

[1] Department of Applied Chemistry, Graduate School of Engineering, Osaka Prefecture University, 1-1 Gakuen-cho, Naka-ku, Sakai, Osaka 599-8531, Japan

Scheme 1 Alternating copolymerization of MMI and isobutene

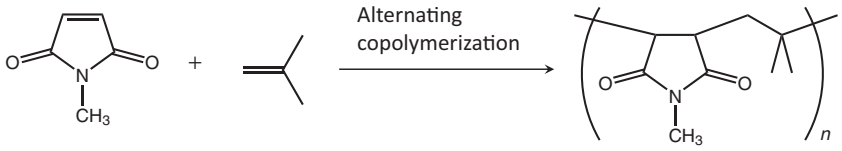

Scheme 2 AAB sequence-controlled copolymerization of RMI and DIB

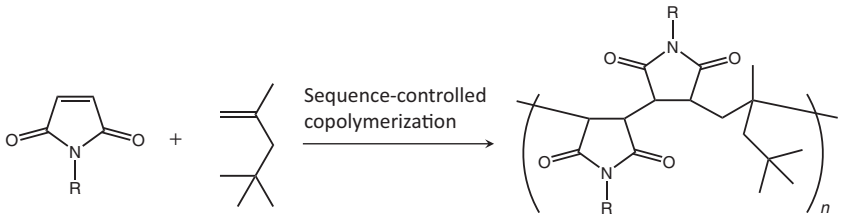

properties (visible light transmittance more than 95%) and well-balanced mechanical properties (flexural strength more than 130 MPa and flexural elasticity more than 4.5 GPa) [33].

Another type of olefin can provide different types of polymers with a controlled sequence structure. When the RMIs are copolymerized with an electron-donating monomer with considerable steric bulkiness, such as limonene (Lim) [34], β-pinene [35], diisobutene (DIB) [36], and 1-methylenebenzocycloheptane [37], AAB sequence-controlled copolymers (…$M_1M_1M_2M_1M_1M_2$…) are produced rather than alternating copolymers, as shown in Scheme 2. A repeating unit before the terminal repeating unit (i.e., penultimate unit (PU) effect) plays an important role in the production of AAB sequence-controlled copolymers. Many studies have been carried out to study the PU effect observed during radical copolymerization [34–54]. For example, Fukuda and coworkers reported their experimental results for copolymerization kinetics using a rotating sector method and kinetic analyses based on their robust theoretical background [40–43]. Davis and Coote et al. also investigated the PU effect using theoretical chemistry [44–48].

The unusual copolymerization behavior of the RMIs has been noted in the literature [55–58]. Recently, the PU effect was investigated in detail for the copolymerization of *N*-phenylmaleimide (PhMI) with various monomers. Satoh et al. reported the synthesis of AAB-type sequence-controlled copolymers with a controlled molecular weight, molecular weight distribution and chain-end structure using reversible addition-fragmentation chain transfer (RAFT) polymerization of PhMI with Lim [34] and other various olefins [38, 39]. Yamamoto et al. revealed the solvent effect on the PU-controlled copolymerization system with PhMI and β-pinene [35]. In that study, solvents with a high Lewis acidity significantly interacted with PhMI. Hisano et al. revealed that the PU control of propagation was significantly dependent on the ring number of 1-methylenebenzocycloalkanes during copolymerization with PhMI [37]. In contrast to the studies on the PU effect during copolymerization using a wide variety of olefins and styrene derivatives, no studies on the role of the N-substituents of the RMIs with regards to the PU effect have been reported. The PU effect may be due to the polar and steric effects of the substituents on the polymers and reacting monomers. However, these effects have not been clarified. In this study, we carried out the radical copolymerization of various kinds of RMIs with DIB and Lim (Fig. 1) and determined the monomer reactivity ratios based on the terminal and PU models to gain insight into the polar, resonance, and steric effects of the substituents.

Experimental methods

Materials

Commercially available PhMI (Wako Pure Chemical Industries, Ltd., Osaka), DIB (Nacalai Tesque, Kyoto), and Lim (Nacalai Tesque, Kyoto) was used after recrystallization or distillation. The other RMIs (i.e., MMI, *N*-cyclohexylmaleimide (CHMI), *N*-*tert*-butylmaleimide (tBMI), *N*-*tert*-octylmaleimide (tOMI), *N*-acetylmaleimide (AcMI), *N*-(4-methylphenyl)maleimide (4MPhMI), *N*-(2-methylphenyl) maleimide (2MPhMI), *N*-(2-ethylphenyl)maleimide (2EPhMI), *N*-(2,6-diethylphenyl)maleimide (2,6DEPhMI), *N*-(4-methoxyphenyl)maleimide (4MOPhMI), and *N*-(4-ethoxy carbonylphenyl)maleimide (4ECPhMI)) were synthesized from maleic anhydride and the corresponding amines according to previously reported methods [28]. 2,2′-Azobis-(isobutyronitrile) (AIBN, Wako Pure Chemical Industries, Ltd., Osaka) was recrystallized from methanol. All solvents were distilled prior to use.

General procedures

Size exclusion chromatography (SEC) was carried out using Chromatoscience CS-300C, JASCO PU-2080PLUS, JASCO DG-2080-53, JASCO RI-2031-PLUS, TOSOH

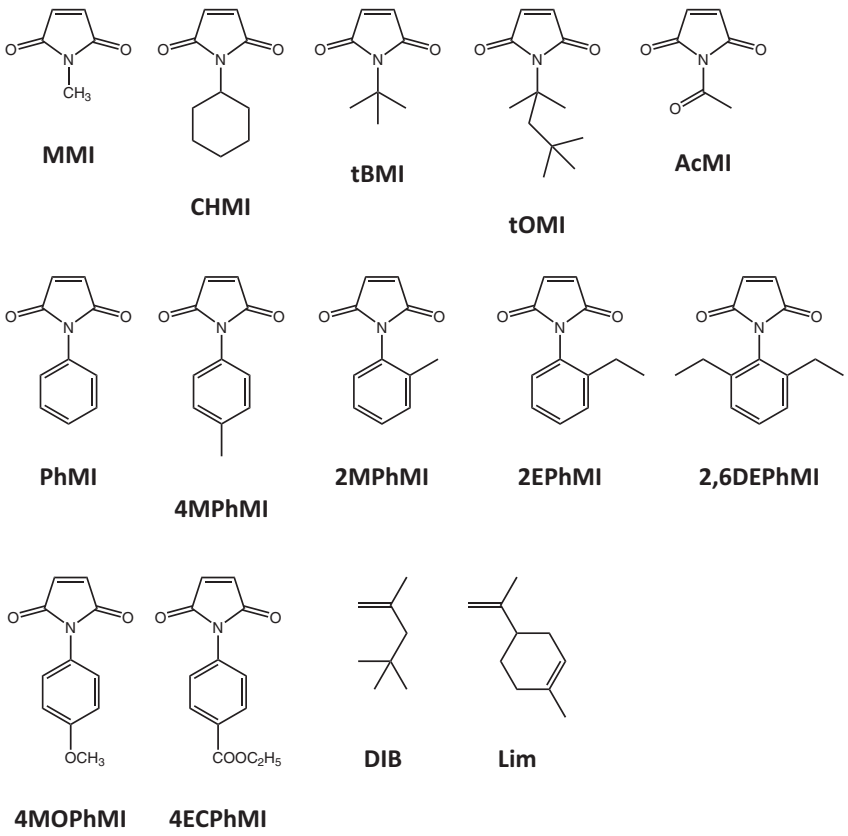

Fig. 1 Structures of monomers used in this study

TSK-gel columns, GMH_{HR}-N and GMH_{HR}-H, and tetrahydrofuran (THF) as the eluent. Number- and weight-average molecular weights (M_n and M_w, respectively) as well as polydispersity (M_w/M_n) values were determined by calibration with standard polystyrenes. The NMR spectrum was recorded in $CDCl_3$ using a JEOL ECS-400 spectrometer. The IR and UV-Vis spectra were recorded using JASCO FT-IR410 and Shimadzu UV-2400PC spectrometers, respectively. Thermogravimetric (TG) analysis was carried out using a Shimadzu TGA-50 with a nitrogen stream at a flow rate of 10 mL/min and heating rate of 10 °C/min. DFT calculations were carried out using Spartan'10 (Wave Function, Inc.) at the B3LYP/6-311 G* level.

Copolymerization procedures

Monomers, AIBN, and chloroform were placed in a glass tube. After the freeze–thaw cycles, the solution was heated at a determined temperature for a given time. Then, the polymerization mixture was poured into a large amount of methanol. The precipitated copolymers were filtered, washed, and dried in vacuo. The copolymer yield was gravimetrically determined. The copolymers were purified by precipitation using chloroform and methanol. The composition of the copolymers was determined by ^{1}H NMR spectroscopy. The copolymer compositions of tBMI or tOMI with DIB were calculated based on the monomer consumption during copolymerization by ^{1}H NMR spectroscopy using the peak intensity due to 2,4,4-trimethyl-2-pentene, which is included in DIB as the internal standard. We confirmed the good agreement between the results obtained from the two different methods. The copolymer composition was actually determined by analyses of the ^{1}H NMR spectrum of the resulting copolymer and the monomer consumption during the copolymerization of CHMI and DIB with a 1/1 molar ratio in the feed. The CHMI content in the copolymer was determined to be 56.1 and 55.4 mol% by gravimetric and NMR analyses, respectively.

Determination of monomer reactivity ratios

All the copolymers were recovered at a low conversion to allow for analysis of the copolymerization parameters using the Mayo-Lewis equation (Eq. 1).

$$\frac{d[M_1]}{d[M_2]} = \frac{[M_1](r_1[M_1] + [M_2])}{[M_2](r_2[M_2] + [M_1])} \quad (1)$$

The monomer reactivity ratios (i.e., r_1 and r_2) were determined by the terminal and PU models.

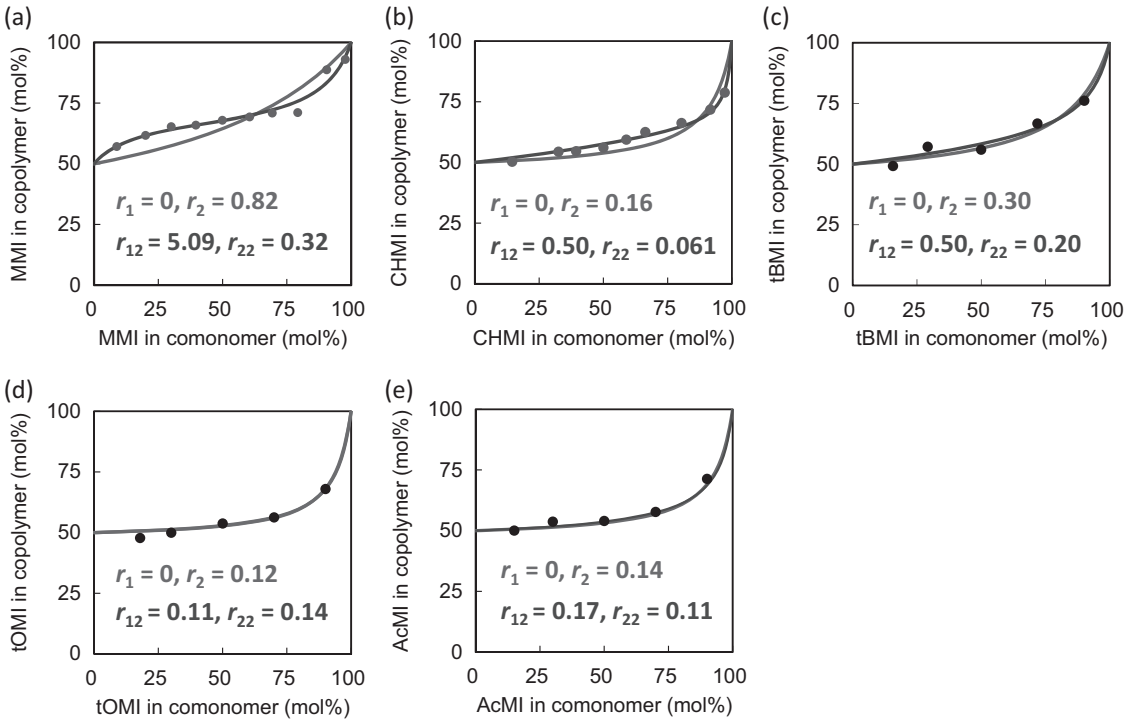

Fig. 2 Comonomer–copolymer composition curves for the radical copolymerization of **a** MMI, **b** CHMI, **c** tBMI, **d** tOMI, and **e** AcMI (M_2) with DIB (M_1). Red and blue indicate the results analyzed using the terminal and PU models, respectively

For the terminal model, the r_1 and r_2 values are defined by Eqs. 2 and 3, respectively.

$$r_1 = k_{11}/k_{12} \tag{2}$$

$$r_2 = k_{22}/k_{21} \tag{3}$$

The Fineman-Ross [59] and Kelen-Tüdõs [60] methods yielded scattered plots, and the calculated comonomer–copolymer composition curves did not fit the experimental data in several cases (See Supporting Information). In contrast, the curve-fitting method using the nonlinear least-squares procedure resulted in good results over the nonlinear least-squares method entire range of compositions [37].

In general, the penultimate unit model involves the use of eight propagation reactions with four monomer reactivity ratios (Eqs. 4–7)

$$r_{11} = k_{111}/k_{112} \tag{4}$$

$$r_{12} = k_{122}/k_{121} \tag{5}$$

$$r_{21} = k_{211}/k_{212} \tag{6}$$

$$r_{22} = k_{222}/k_{221} \tag{7}$$

With these four monomer reactivity ratios, the copolymer composition can be represented as shown in Eq. 8.

$$f = \frac{1 + r_{21}F\left(\frac{r_{11}F+1}{r_{21}F+1}\right)}{1 + \frac{r_{12}}{F}\left(\frac{r_{22}+F}{r_{12}+F}\right)} \tag{8}$$

where $F = [M_1]/[M_2]$ and $f = d[M_1]/d[M_2]$. In this case, the r_{11} and r_{21} values are zero due to the lack of homopolymerization ability. Therefore, Eq. 8 can be reformulated as Eq. 9.

$$\frac{1-2f}{F(1-f)} = \frac{f}{F^2(1-f)}r_{22} - \frac{1}{r_{12}} \tag{9}$$

Results and discussion

First, we investigated the PU effect for the copolymerization of MMI, CHMI, tBMI, and tOMI (M_2) with DIB (M_1) to discuss the steric effect of the *N*-alkyl groups. The comonomer–copolymer composition curves are shown in Fig. 2. The monomer reactivity ratios were calculated based on the terminal and PU models using the nonlinear least-squares method. The largest PU effect was observed

Table 1 Monomer reactivity ratios and kinetic parameters for the radical copolymerization of RMIs with *N*-alkyl substituents (M_2) with DIB (M_1)

RMI (M_2)	E_s^a	$r_2^b(=k_{22}/k_{21})$	$r_{12}^c(=k_{122}/k_{121})$	$r_{22}^c(=k_{222}/k_{221})$	r_{12}/r_{22}	$R_p \times 10^5$ (L/mol·s)	k_p ($=k_{222}$) (mol/L·s)	k_{221} (mol/L·s)
MMI	−1.30	0.82	5.09	0.32	15.7	–	–	–
CHMI	−2.09	0.16	0.50	0.061	8.2	–	–	–
tBMI	−2.78	0.30	0.50	0.20	2.6	13.6[d,e]	100[e]	500
tOMI	−5.14	0.12	0.11	0.14	~1	2.69[d,e]	23[e]	160
AcMI	–	0.14	0.17	0.11	1.5	–	–	–

[a]For the N-substituent of the RMIs

[b]Determined based on the terminal model ($r_1 = 0$)

[c]Determined based on the PU model ($r_{11} = r_{21} = 0$)

[d]Polymerization conditions: [RMI] = 1 mol/L, [AIBN] = 5 mmol/L in benzene at 60 °C

[e]Cited from ref. [62]

in the copolymerization of MMI. The curve based on the terminal model did not provide a good representation of the experiment data. However, the curve considering the PU effect provide a good representation of the experimental data over the entire range of comonomer compositions in the feed, as shown in Fig. 2a. In contrast, the PU effect was negligible for the copolymerization of tOMI containing the most sterically hindered N-substituent. In this case, the r_1 value that was determined using the terminal model as well as the r_{12} and r_{22} values that were determined using the PU model were in agreement (Fig. 2d). The copolymerizations of CHMI and tBMI exhibited an intermediate reaction behavior (i.e., a weak PU effect was observed) (Fig. 2b, c).

In Table 1, we summarize the reactivity and kinetic parameters for these copolymerization systems. The E_s parameter is the Taft's steric factor, which is represented as a negative value according to its steric bulkiness [61]. The larger absolute value indicates the larger steric hindrance. In this study, the steric bulkiness of the N-substituent was in the order of methyl < cyclohexyl < *tert*-butyl < *tert*-octyl groups. The r_{12}/r_{22} value indicates the magnitude of the PU effect. A larger PU effect was observed for larger r_{12}/r_{22} values. When no PU effect was observed during copolymerization, the r_{12}/r_{22} value is equal to unity. The largest r_{12}/r_{22} value was observed for the copolymerization of MMI, and this value decreased as the steric bulkiness of the N-substituents increased. Here, we can evaluate the absolute value of k_{221} using the r_{22} value determined in this study along with the k_p ($=k_{222}$) value reported in the literature [62]. As the bulkiness of the N-substituent increased, the k_{221} values decreased. This result suggests that significant steric hindrance is present between the N-substituents and the bulky olefin monomer when the propagating radical includes successive RMI repeating units (Fig. 3). In addition, the contribution of the polar effect on the PU control was investigated. The r_{12}/r_{22} value for AcMI with an electron-accepting N-substituent was one tenth that for MMI with an electron-donating substituent. The PU effect was not observed for copolymerization of AcMI (Fig. 2e), which is in contrast to the significant PU effect observed for copolymerization of MMI. This result indicates that the introduction of an electron-withdrawing group is disadvantageous for induction of the PU effect.

Fig. 3 Image for steric repulsion between the ~RMI-RMI radical and an olefin monomer

Previously, significant steric hindrance has been observed for the radical polymerization of *N*-(substituted phenyl)maleimides and their copolymerization with styrene and methyl methacrylate [30]. Therefore, the steric effect of the alkyl substituents that are included in an *N*-phenyl moiety was investigated. In this study, we carried out the copolymerization of 4MPhMI, 2MPhMI, 2EPhMI, and 2,6DEPhMI (M_2) with DIB (M_1). The comonomer–copolymer composition curves calculated by the terminal and PU models are shown in Fig. 4.

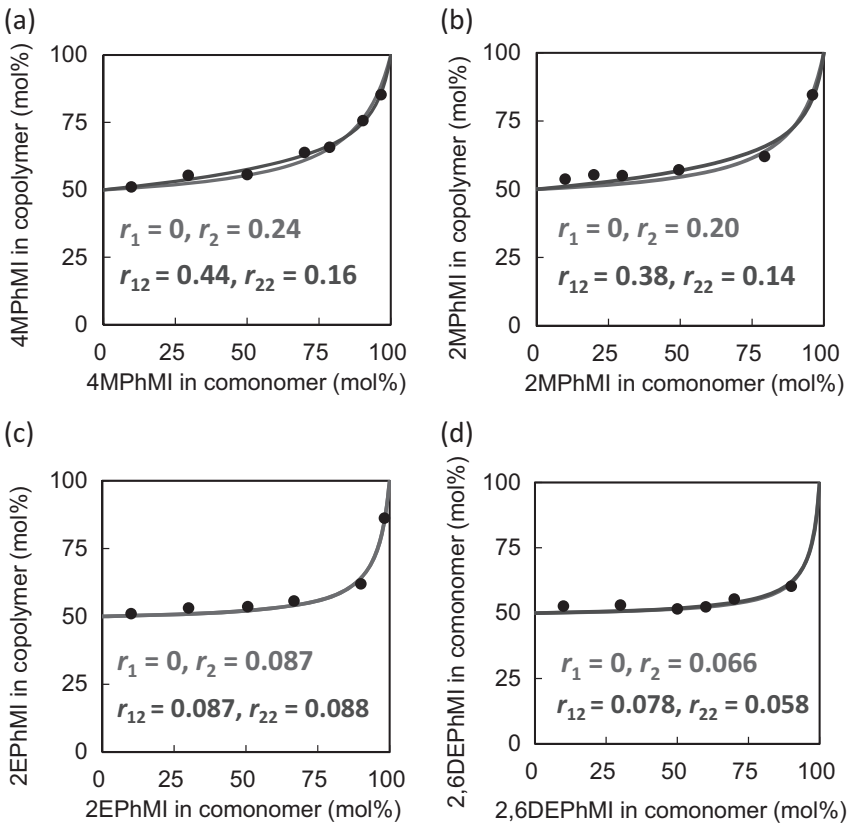

Fig. 4 Comonomer–copolymer composition curves for the radical copolymerization of **a** 4MPhMI, **b** 2MPhMI, **c** 2EPhMI, and **d** 2,6DEPhMI (M_2) with DIB (M_1). Red and blue indicate the results analyzed using the terminal and PU models, respectively

For these copolymerizations, the curves using the terminal and PU models were similar, and both methods provided a good representation of the experimental data. The r_{12} and r_{22} values computed from the results of the curve fitting process using the PU model were close to the r_1 value determined from the terminal model. Therefore, the PU effect was much smaller during the copolymerization of these *N*-(alkylphenyl)maleimides. The r_{12}/r_{22} value was 2.8 for 4MPhMI and 2MPhMI but close to unity for 2EPhMI and 2,6DEPhMI. To achieve 2:1 sequence control, the ~DIB-RMI radical should attack RMI rather than DIB, and the produced ~RMI-RMI radical must selectively react with DIB. Based on analysis of propagation rate constants [63, 64], the bulky N-substituent decreases the rate of both reactions. Due to an increase in the steric bulkiness of the alkyl substituents at the ortho position of the *N*-phenyl group, the k_p value (and the k_{221} value) rapidly decreased. In addition, the overall polymerization rate decreased [64] (Table 2). The alternating tendency increased with an increase in the steric bulkiness due to a decrease in the homopropagation rate. The decrease in the k_p ($= k_{222}$) value was greater than that of the k_{221} value due to increased steric repulsion during homopropagation.

A change in the reactivity is correlated to direct steric hindrance and the molecular conformation that accompanies the twisted structure between the maleimide and *N*-phenyl rings [65–67]. Figure 5 shows the most stable molecular conformation for 4MPhMI and 2EPhMI. These conformations were optimized using DFT calculations. The distorted conformation arises from the steric repulsion between the ortho-alkyl groups of the *N*-phenyl ring and the carbonyl groups of the maleimide ring. The observed spectral data and DFT results support the twisted conformation of the ortho-substituted RMIs. The torsion angles between the maleimide and phenyl rings were 47.0 and 76.9°, and the HOMO–LUMO gaps were 4.04 and 3.64 eV for 4MPhMI and 2EPhMI, respectively. These calculated results were in good agreement with their UV spectral data. The observed λ_{max} values were 312 and 293 nm for 4MPhMI and 2EPhMI, respectively. These twisted structures suppress the monomer reactivity due to the reduced resonance effect. Therefore, the high alternating tendency masked the PU effect.

It is important to note that the appearance of the PU effect is dependent on the steric bulkiness of the olefins. No PU effect was observed during copolymerization of PhMI and other RMIs with isobutene. However, a significant PU effect was observed during copolymerization of PhMI with Lim [34], which has a bulky rigid structure. In addition, copolymerizations with DIB exhibited intermediate copolymerization features [36]. Olefins with a bulky and rigid molecular structure exhibited a larger PU effect during the copolymerization of PhMI. For example, using the r_{12} and

Table 2 Monomer reactivity ratios and kinetic parameters for the radical copolymerization of RMIs with *N*-alkylphenyl substituents (M_2) with DIB and Lim (M_1)

Olefin (M_1)	RMI (M_2)	σ_p^a	$r_2^b(=k_{22}/k_{21})$	$r_{12}^c(=k_{122}/k_{121})$	$r_{12}^c(=k_{122}/k_{221})$	r_{12}/r_{22}	$R_p^{d,e} \times 10^5$(L/mol · s)	$k_p^d(=k_{222})$ (mol/L · s)	k_{221} (mol/L·s)
DIB	PhMI	0	0.16	0.18	0.15	1.2	–	–	–
DIB	4MPhMI	−0.17	0.24	0.44	0.16	2.8	11.4[f]	1200[f]	7500
DIB	2MPhMI	–	0.20	0.38	0.14	2.8	5.15	190	1500
DIB	2EPhMI	–	0.087	0.087	0.088	1.0	–	–	–
DIB	2,6DEPhMI	–	0.066	0.078	0.058	1.4	0.401	2.0	34
DIB	4ECPhMI	0.45	0.17	0.23	0.12	1.9	–	–	–
DIB	4MOPhMI	−0.27	0.42	0.58	0.37	1.6	–	–	–
Lim	PhMI	0	1.0	6.2	0.42	15	–	–	–
Lim	4MPhMI	−0.17	1.9	13	0.56	23	11.4[f]	1200[f]	2100
Lim	4MOPhMI	−0.27	1.9	35	0.77	45	–	–	–

[a]Substituent constant for the Hammett plot (Ref. [61]). Here, the value corresponds to the *p*-substituent on the *N*-phenyl group

[b]Determined based on the terminal model ($r_1 = 0$)

[c]Determined based on the PU model ($r_{11} = r_{21} = 0$)

[d]Cited from refs. [63, 64]

[e]Polymerization conditions: [RMI] = 1 mol/L, [AIBN] = 5 mmol/L in benzene at 60 °C

[f]Data for *N*-(4-ethylphenyl)maleimide. Cited from refs. [63]

r_{22} values reported in the literature, the r_{12}/r_{22} values were calculated to be 9.0 and 69 for the copolymerization systems with 1-vinylcyclohexane and PhMI in dichloromethane and $C_6H_5C(CF_3)_2OH$, respectively [39]. Similarly, the r_{12}/r_{22} values increased to 119 and 120 for the copolymerizations of 3-vinylcyclohexene and 3-isopropenylcyclohexene, respectively. The enhanced PU effect reflects the significant steric hindrance due to the rigid olefin structures, and the steric hindrance in the RMIs was not favored as described above.

In addition to the steric effect, the polar effect was investigated for the RMIs with substituents at the para position of PhMI (i.e., 4ECPhMI, 4MPhMI, and 4MOPhMI). The r_{12}/r_{22} values were as small as 1.2–2.8 during copolymerization with DIB. Therefore, the PU effect was studied for RMIs including the polar groups using copolymerization with Lim as the comonomer. Satoh et al. reported that Lim induced large PU effects for copolymerization with PhMI [34]. However, no data are available on the polar effect of RMIs. The bulky rigid structure of the olefin monomers is expected to enhance the PU effect. As shown in Fig. 6 and Table 2, the r_{12}/r_{22} values were determined to be 45, 23, and 15 for the copolymerizations of 4MOPhMI, 4MPhMI, and PhMI, respectively. The order of the magnitude of the effect was in agreement with the order of the electron-donating properties of the substituents. Yamamoto et al. previously reported a significant solvent effect during radical copolymerization of PhMI with *β*-pinene [35]. When the Lewis acidity of the solvent increased, the PU effect increased. For example, the r_{12}/r_{22} values increased in the following order: 29 in tetrahydrofuran, 44 in 1,2-dichloroethane, 78 in 2,2,2-trifluoroethanol, and 560 in perfluoro-*tert*-butanol [35]. An increase in the Lewis acidity can enhance the interaction between the carbonyl group of the RMIs and the solvent molecules, leading to an increase in steric hindrance around the RMIs. The electron-donating N-substituent may assist the RMI-solvent interaction due to an increase in the electron density on the oxygen atom of the carbonyl groups, which leads to enhancement of the PU effect.

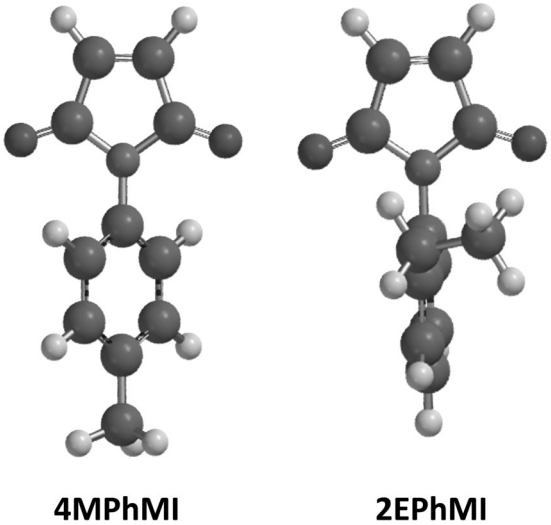

Fig. 5 Molecular models for 4MPhMI and 2EPhMI based on DFT calculations

Conclusion

In this study, we investigated the influence of steric, resonance, and polar effects of N-substituents on sequence

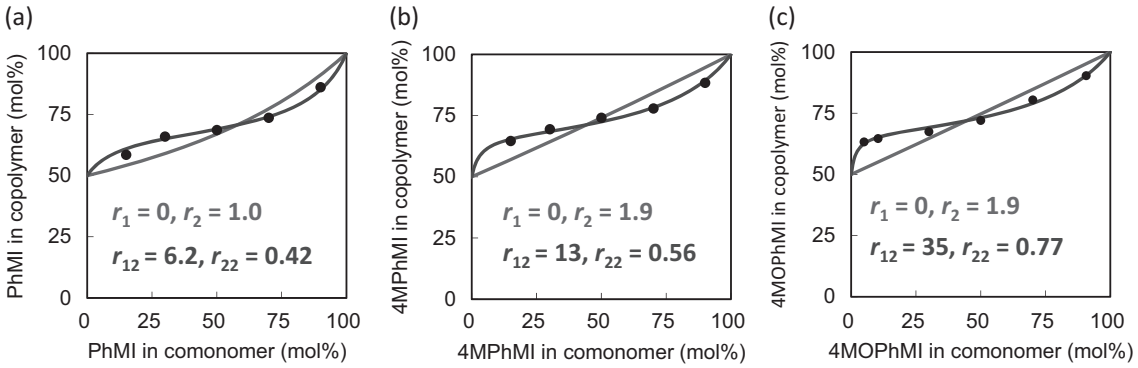

Fig. 6 Comonomer–copolymer composition curves for the radical copolymerization of **a** PhMI, **b** 4MOMI, and **c** 4MPhMI (M_2) with Lim (M_1). Red and blue indicate the results analyzed using the terminal and PU models, respectively

control during radical copolymerization of RMIs with DIB and Lim in chloroform at 60 °C. The monomer reactivity ratios (i.e., r_2 ($= k_{22}/k_{21}$) based on the terminal model as well as r_{12} ($= k_{122}/k_{121}$) and r_{22} ($= k_{222}/k_{221}$) based on the PU model) were determined. When the steric effect was studied using RMIs with bulky *N*-alkyl substituents, the PU effect was suppressed due to steric hindrance, leading to the formation of alternating copolymers with DIB. The introduction of bulky substituents at the ortho position of *N*-phenylmaleimides also predominantly caused alternating copolymer formation. However, the polar effect was observed during copolymerization of *N*-phenylmaleimides including various para-substituents with DIB and Lim. Therefore, less bulky and more electron-donating substituents that were introduced in the RMIs enhanced the PU effect for radical copolymerization of the RMIs with olefins. We have demonstrated that 2:1 sequence-controlled maleimide copolymers can be efficiently produced during radical copolymerization of Lim and *N*-phenylmaleimides with an electron-donating substituent at the 4-position of the *N*-phenyl group.

Compliance with ethical standards

Conflict of interest The authors declare that they have no conflict of interest.

Publisher's note: Springer Nature remains neutral with regard to jurisdictional claims in published maps and institutional affiliations.

References

1. Matyjaszewski K, Müller M, Coates GW, Sawamoto M, (Eds.). Polymer science: A comprehensive reference, chain polymerization of vinyl monomers. Vol. 3. Amsterdam: Elsevier; 2012.
2. Matyjaszewski K. Atom transfer radical polymerization (ATRP): current status and future perspectives. Macromolecules 2012;45:4015–39.
3. Nicolas J, Guillaneuf Y, Lefay C, Bertin D, Gigmes D, Charleux B. Nitroxide-mediated polymerization. Prog Polym Sci. 2013;38:63–235.
4. Ouchi M, Sawamoto M. Metal-catalyzed living radical polymerization: discovery and perspective. Macromolecules 2017;50:2603–14.
5. Chmielarz P, Fantin M, Park S, Isse AA, Gennaro A, Magenau AJD. et al. Electrochemically mediated atom transfer radical polymerization (eATRP). Prog Polym Sci. 2017;69:47–78.
6. Moad G. RAFT polymerization to form stimuli-responsive polymers. Polym Chem 2017;8:177–219.
7. Lutz JF, Lehn JM, Meijer EW, Matyjaszewski K. From precision polymers to complex materials and systems. Nat Rev Mater 2016;1:5. https://doi.org/10.1038/natrevmats.2016.24
8. Pelegri-O'Day EM, Maynard HD. Controlled radical polymerization as an enabling approach for the next generation of protein-polymer conjugates. Acc Chem Res. 2016;49:1777–85.
9. Boyer C, Corrigan NA, Jung K, Diep N, Thuy-Khanh N, Adnan NNM. et al. Copper-mediated living radical polymerization (Atom transfer radical polymerization and Copper(0) mediated polymerization): From fundamentals to bioapplications. Chem Rev. 2016;116:1803–949.
10. Anastasaki A, Nikolaou V, Nurumbetov G, Wilson P, Kempe K, Quinn JF. et al. Cu(0)-mediated living radical polymerization: a versatile tool for materials synthesis. Chem Rev. 2016;116:835–77.
11. Derry MJ, Fielding LA, Armes SP. Polymerization-induced self-assembly of block copolymer nanoparticles via RAFT non-aqueous dispersion polymerization. Prog Polym Sci. 2016;52:1–18.
12. Satoh K, Kamigaito M. Stereospecific living radical polymeization: dual control of chain length and tacticity for precision polymer synthesis. Chem Rev. 2009;109:5120–56.
13. Noble BB, Coote ML. Mechanistic perspectives on stereocontrol in Lewis acid-mediated radical polymerization: lessons from small-molecule synthesis. Adv Phys Org Chem. 2015;49:189–258.
14. Lutz JF. Sequence-controlled polymerizations: The next Holy Grail in polymer science? Polym Chem 2010;1:55–62.
15. Lutz JF, Ouchi M, Liu DR, Sawamoto M. Sequence-controlled polymers. Science 2013;341:628. https://doi.org/10.1126/science.1238149
16. Hibi Y, Ouchi M, Sawamoto M. A strategy for sequence control in vinyl polymers via iterative controlled radical cyclization. Nat Commun 2016;7:11064.

17. Ouchi M, Sawamoto M. Sequence-controlled polymers via reversible-deactivation radical polymerization. Polym J 2018;50:83–94.
18. Terashima T, Mes T, De Greef TFA, Gillissen MAJ, Besenius P, Palmans ARA. et al. Single-chain folding of polymers for catalytic systems in water. J Am Chem Soc. 2011;133:4742–5.
19. De Neve J, Haven JJ, Maes L, Junkers T. Sequence-definition from controlled polymerization: the next generation of materials. Polym Chem 2018;9:4692–705.
20. Serizawa T, Akashi M. Stereoregular polymerization with template nanospaces. Polym J 2006;38:311–28.
21. Ajiro H, Kamei D, Akashi M. Mechanistic Studies on template polymerization in porous isotactic-poly(methyl methacrylate) thin films by radical polymerization and postpolymerization of methacrylate derivatives. Macromolecules 2009;42:3019–25.
22. Ida S, Ouchi M, Sawamoto M. Template-assisted selective radical addition toward sequence-regulated polymerization: lariat capture of target monomer by template initiator. J Am Chem Soc 2010;132:14748–50.
23. Soejima T, Satoh K, Kamigaito M. Monomer sequence regulation in main and side chains of vinyl copolymers: synthesis of vinyl oligomonomers via sequential atom transfer radical addition and their alternating radical copolymerization. ACS Macro Lett 2015;4:745–9.
24. Soejima T, Satoh K, Kamigaito M. Main-chain and side-chain sequence-regulated vinyl copolymers by iterative atom transfer radical additions and 1:1 or 2:1 alternating radical copolymerization. J Am Chem Soc 2016;138:944–54.
25. Ojika M, Satoh K, Kamigaito M. BAB-random-C monomer sequence via radical terpolymerization of limonene (A), maleimide (B), and methacrylate (C): terpene polymers with randomly distributed periodic sequences. Angew Chem Int Ed 2017;56:1789–93.
26. Cowie JMG. Alternating copolymers. New York: Plenum Press; 1985.
27. Hirooka M, Yabuuchi H, Morita S, Kawasumi S, Nakaguchi K. Complex copolymerization. I. Novel equimolar copolymers of acrylonitrile and olefins. J Polym Sci Part B Polym Lett 1967;5:47–55.
28. Cubbon RCP. The free radical and anionic polymerization of some N-substituted maleimides. Polymer 1965;6:419–26.
29. Barrales-Rienda JM, De la Campa JIG, Ramos JG. Free-radical copolymerizations of *N*-phenylmaleimide. J Macromol Sci Part A Chem 1977;A11:267–86.
30. Matsumoto A, Kubota T, Otsu T. Radical polymerization of *N*-(alkyl-substituted phenyl)maleimides: synthesis of thermally stable polymers soluble in nonpolar solvents. Macromolecules 1990;23:4508–13.
31. Otsu T, Matsumoto A, Kubota T. Increase in thermal stability of vinyl polymers through radical copolymerization with *N*-cyclohexylmaleimide. Polym Int 1991;25:179–84.
32. Matsumoto A. Sequence-controlled radical copolymerization for the design of high-performance transparent polymer materials. ACS Symp Ser 2014;1170:301–12.
33. Doi T, Akimoto A, Matsumoto A, Otsu T. Radical copolymerization of *N*-alkylmaleimides with isobutene and the properties of the resulting alternating copolymers. J Polym Sci Part A Polym Chem 1996;34:367–73.
34. Satoh K, Matsuda M, Nagai K, Kamigaito M. AAB-sequence living radical chain copolymerization of naturally occurring limonene with maleimide: an end-to-end sequence-regulated copolymer. J Am Chem Soc 2010;132:10003–5.
35. Yamamoto D, Matsumoto A. Penultimate unit and solvent effects on 2:1 sequence control during radical copolymerization of N-phenylmaleimide with β-pinene. Macromol Chem Phys 2012;213:2479–85.
36. Hisano M, Takeda K, Takashima T, Jin Z, Shiibashi A, Matsumoto A. Sequence controlled radical copolymerization of N-substituted maleimides with olefins and polyisobutene macromonomers to fabricate thermally stable and transparent maleimide copolymers with tunable glass transition temperatures and viscoelastic properties. Macromolecules 2013;46:7733–44.
37. Hisano M, Takeda K, Takashima T, Jin Z, Shiibashi A, Matsumoto A. Sequence controlled radical polymerization of N-substituted maleimides with 1-methylenebenzocycloalkanes and the characterization of the obtained copolymers with excellent thermal resistance and transparency. Macromolecules 2013;46:3314–23.
38. Matsuda M, Satoh K, Kamigaito M. Periodically functionalized and grafted copolymers via 1:2-sequence-regulated radical copolymerization of naturally occurring functional limonene and maleimide derivatives. Macromolecules 2013;46:5473–82.
39. Matsuda M, Satoh K, Kamigaito M. 1:2-sequence-regulated radical copolymerization of naturally occurring terpenes with maleimide derivatives in fluorinated alcohol. J Polym Sci Part A Polym Chem 2013;51:1774–85.
40. Fukuda T, Kubo K, Ma YD. Kinetics of free radical copolymerization. Prog Polym Sci. 1992;17:875–916.
41. Fukuda T, Goto A, Kwak Y, Yoshikawa C, Ma YD. Penultimate unit effects in free radical copolymerization. Macromol Symp 2002;182:53–64.
42. Fukuda T, Ma YD, Kubo K, Inagaki H. Penultimate-unit effects in free-radical copolymerization. Macromolecules 1991;24:370–5.
43. Ma YD, Sung KS, Tsujii Y, Fukuda T. Free-radical copolymerization of styrene and diethyl fumarate. Penultimate-unit effects on both propagation and termination processes. Macromolecules 2001;34:4749–56.
44. Coote ML, Davis TP. The mechanism of the propagation step in free-raidcal copolymerisation. Prog Polym Sci. 1999;24:1217–51.
45. Coote ML, Johnston LPM, Davis TP. Copolymerization propagation kinetics of styrene and methyl methacrylate-revisited. 2. Kinet Anal Macromol 1997;30:8191–204.
46. Coote ML, Davis TP, Radom L. Effect of the penultimate unit on radical stability and reactivity in free-radical polymerization. Macromolecules 1999;32:2935–40.
47. Coote ML, Krenske EH, Izgorodina EI. Computational studies of RAFT polymerization: mechanistic insights and practical applications. Macromol Rapid Commun. 2006;27:473–97.
48. Lin C, Coote ML, Petit A, Richard P, Poli R, Matyjaszewski K. Ab initio study of the penultimate effect for the ATRP activation step using propylene, methyl acrylate, and methyl methacrylate monomers. Macromolecules 2007;40:5985–94.
49. Davis TP, O'Driscoll KF, Piton MC, Winnik MA. Copolymerization propagation kinetics of styrene with alkyl acrylates. Polym Int 1991;24:65–70.
50. Burke AL, Duever TA, Penlidis A. Discriminating between the terminal and penultimate models using designed experiments: an overview. Ind Eng Chem Res 1997;36:1016–35.
51. Buback M, Feldermann A, Barner-Kowollik C, Lacik I. Propagation rate coefficients of acrylate-methacrylate free-radical bulk copolymerizations. Macromolecules 2001;34:5439–48.
52. Madruga EL. From classical to living/controlled statistical free-radical copolymerization. Prog Polym Sci. 2002;27:1879–924.
53. Klumperman B. Mechanistic considerations on styrene-maleic anhydride copolymerization reactions. Polym Chem 2010;1:558–62.
54. Schier JES, Cohen-Sacal D, Hutchinson RA. Hydrogen bonding in radical solution copolymerization kinetics of acrylates and methacrylates: a comparison of hydroxy- and methoxy-functionality. Polym Chem 2017;8:1943–52.
55. Florjanczyk Z, Krawiec W, Such K. A study of the relative reactivity of maleic anhydride and some maleimides in free radical copolymerizatin and terpolymerization. J Polym Sci Part A Polym Chem 1990;28:795–801.

56. Matsumoto A, Hiuke R, Doi T. Evident solvent effect on propagation reactions during radical copolymerization of maleimide and alkene. J Polym Sci Part A Polym Chem 1997;35:1515–25.
57. Nair CPR, Mathew D, Ninan KN. Free radical copolymerization of *N*-(4-hydroxyphenyl)maleimide with vinyl monomers: solvent and penultimate-unit effects. Eur Polym J 1999;35:1829–40.
58. Wang Y, Chen Q, Liang H, Lu J. Conventional and RAFT radical copolymerization of β-pinene with N-substituted maleimides. Polym Int 2007;56:1514–20.
59. Finemann M, Ross SD. Linear method for determining monomer reactivity ratios in copolymerization. J Polym Sci 1950;5:259–62.
60. Kelen T, Tüdõs F. Analysis of the linear methods for determining copolymerization reactivity ratios. I. A new improved linear graphic method. J Macromol Sci Chem 1975;A9:1–27.
61. Hansch C, Leo LJ. Substituent constants for correlation analysis in chemistry and biology. New York: John Wiley & Sons; 1979.
62. Matsumoto A, Oki Y, Otsu T. Propagation and termination rate constants of *N-tert*-alkyl- and *N*-trialkysilylmaleimides in radical polymerization initiated with 2,2′-azobisisobutyronitrile. Polym J 1993;25:237–43.
63. Matsumoto A, Oki Y, Otsu T. Steric effect of alkyl substituents on propagation rate constants of *N*-(2,6-dialkylphenyl)maleimides in radical polymerization. Macromolecules 1992;25:3323–4.
64. Matsumoto A, Oki Y, Otsu T. Effects of the substituents on radical polymerization kinetics of *N*-(alkyl-substituted phenyl) maleimides initiated with dimethyl 2,2′-azobisisobutyrate. Eur Polym J 1993;29:1225–9.
65. Matsuo T. Nature of the longest wavelength absorption bands of *N*-substituted maleimides. Bull Chem Soc Jpn 1965;38: 557–62.
66. Curran DP, Qi H, Geib SJ, DeMello NC. Atroposelective thermal reactions of axially twisted amides and imides. J Am Chem Soc 1994;116:3131–2.
67. Curran DP, Geib SJ, DeMello NC. Rotational features of carbon-nitrogen bonds in *N*-arylmaleimides. Atroposelective reactions of *o-tert*-butylphenylmaleimides. Tetrahedron 1999;55:5681–704.